

Theoretical study of a π -stacking interaction in carbonic anhydrase

MUHAMAD KOYIMATU^a, HIDETO SHIMAHARA^b, KAZUTOMO KAWAGUCHI^a, HIROSAKI SAITO^a,
KIMIKAZU SUGIMORI^a, AND HIDEKI NAGAO^a

^aInstitute of Science and Engineering, Kanazawa University, Kakuma, Kanazawa 920-1192
Japan, E-mail: koyimatu@wiron1.s.kanazawa-u.ac.jp

^bCenter for Nano Materials and Technology, Japan Advanced Institute of Science and
Technology, Nomi, Ishikawa 923-1292 Japan, E-mail: shim@jaist.ac.jp

Abstract.

Human carbonic anhydrase II (HCA II) catalyses the reversible hydration of CO₂. In this enzyme, the imidazole ring of histidine at position 64 (His64) functions to transfer the productive proton from the zinc-bound water to the buffer molecule in bulk-water. X-ray data of HCA II show that His64 has two types of side chain orientations, "in" and "out", representing the direction of the imidazole ring toward and away from the active site, respectively. Maupin et al. reported that the imidazole of His64 can be rotated in a model system of the active site to clarify the proton transfer of catalytic mechanism. However, the indole ring of tryptophan at position 5 (Trp5) that is located near the "out" of the imidazole ring of His64 was not considered in the model system. In this study, in order to estimate detailed rotational properties of His64, we constructed two His64-containing models with and without Trp5, and then simulate the constructed structures by using MP2 method and 6-311++G(d,p) basis sets. This allows us to tentatively determine the potential energies of the π -stacking interaction of the imidazole with the indole in relation to the side chain rotation of His64. The result indicates that the π -stacking interaction causes an increase of the energy barrier between "in" and "out" conformations, implying that the rotational motion of His64 is not relevant to explain the proton transfer during catalysis. Alternatively, a steady position of His64 would be needed in the proton transfer in catalytic mechanism of HCA II.

Keywords: carbonic anhydrase, π -stacking, energy profile, MP2

1 Introduction

Carbonic anhydrase (CA) can be found in plants, animals including human, and certain bacteria. CA is the zinc-containing enzyme that catalyses the reversible hydration of carbon dioxide to form bicarbonate and an excess proton (Equation 1)[1].



The role of the zinc ion in the enzyme is explained through the two-step mechanism[2, 3]. In the first step, the zinc-bound hydroxide binds to the carbon dioxide to form the zinc-bound bicarbonate. The bicarbonate of this intermediate is replaced by a water molecule. In the second step, the zinc-bound hydroxide is regenerated by transferring a proton from the zinc-bound water molecule to an exogenous proton acceptor such as buffer in solution.

Human CA II (HCA II) has 10^6 s^{-1} of the maximal turnover rate[4, 5] that is the fastest value among those of CA isozymes. A kinetic study shows that the maximal rate of a mutant, in which His64 is replaced by another residue, decreases to the similar value to isozymes[6, 7]. The X-ray crystallographic data of HCA II shows that the distance between the imidazole ring of His64

and the zinc-bound water is approximately 7.5Å in the active site, and several water molecules are visible between them. Therefore, His64 is accepted to facilitate the transfer of the productive proton from the zinc-bound water to a buffer molecule in bulk-water through intervening hydrogen bonded water molecules. Many researchers have focused on drawing the mechanism of the proton transfer of HCA II.

For a long time, the final step of the proton transfer (the release of the proton from His64 to buffer) has been assumed to be connected with a rotational or swinging motion of the side chain of His64 because this residue has two conformations, "in" and "out", representing the direction of the imidazole ring toward and away from the active site[8] between the "in" and the "out". Maupin *et al.* supported that this conformational change might occur in the catalysis by using molecular dynamics simulations of a model system[9]. However, the indole of Trp5 has not been considered in the model system. According to the crystal structure, the indole ring of Trp5 parallels to the imidazole ring of "out" conformation of His64 in an off-centered structure, in which a face-to-face or π -stacking interaction should be formed to stabilize the two aromatic rings, as pointed out by Silverman and McKenna[10]. In addition, Riccardi *et al.*[11] and Shimahara *et al.*[12] suggested that the orientation of His64 need not influence the proton release. Mikulski *et al.*[13] also supported it, using kinetic and X-ray methods. Therefore, the possibility that the indole ring of Trp5 interrupts the rotational motion of His64 remains.

In this study, in order to verify whether there is the interruption *via* the π -stacking interaction or not, we constructed two His64-containing models with and without Trp5. The goal of our study is to clarify the detailed mechanism of catalysis.

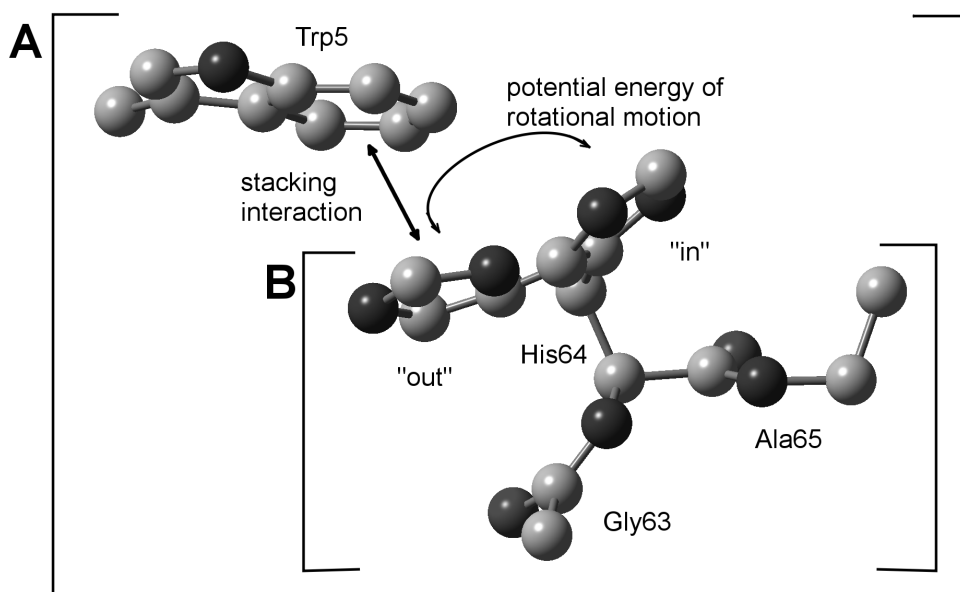


Figure 1: **A.** A model of Gly63-His64-Ala65 structure with Trp5 (Model A). **B.** A model of Gly63-His64-Ala65 structure without Trp5 (Model B). When the imidazole ring passes above the main chain axis consisting of the Gly63-His64-Ala65 by rotation ($\chi_1 = 0$), there is thought to be the potential energy of rotational motion. When the "out" conformation of His64 is assumed to be stabilized by the indole of Trp5 *via* the π -stacking interaction, a change should be investigated in the potential energy. The potential energy surface of Model A was compared with that of Model B.

2 Methodology

2.1 Model Structures

Two models were constructed to investigate the π -stacking interaction between Trp5 and His64, as shown in Figure 1. The first model (Model A) consists of C β and the indole of Trp5; C α , the carbonyl carbon, and the carbonyl oxygen of Gly63; the "out" conformation of His64; N α , C α , and C β of Ala65. The coordinates were obtained from the protein database (PDB) file of the crystal structure of HCA II (2CBA). The χ_1 angle of the "out" was changed: twelve points of χ_1 angle were manually adjusted (-98.6°, -78.6°, -58.6°, -38.6°, -18.6°, -10.0°, 10.0°, 21.4°, 41.4°, 61.4°, 81.4°, 101.4°). Into these structures, hydrogen atoms were artificially added, and then three forms of imidazole: the positively charged imidazolium, the N $_{\delta 1}$ -H tautomer, the N $_{\epsilon 2}$ -H tautomer were considered. In this study, we are focusing on the N $_{\delta 1}$ -H tautomer. C β and the indole of Trp5 were deleted from Model A to construct the second model (Model B). The same manipulations were performed to Model B (12 structures). Totally, we constructed 24 structures.

2.2 Computational Details

The density-functional theory (DFT) using Becke, three-parameter, Lee-Yang-Parr (B3LYP) method was employed for the structural optimization of the location of hydrogen model systems [15]. During the optimization, hetero atoms (carbon, nitrogen, and oxygen) were fixed. Considering the special interaction between electrons such as the π -stacking, it is necessary to use the electron correlation method. Since B3LYP does not include the electron correlation theory, we used the second-order Møller-Plesset perturbation theory (MP2) to estimate the energy of structure [16, 17]. Thus we performed the two-step calculation to obtain the energies of structures. First, B3LYP/6-31G(d,p) level was employed to optimize the geometry of hydrogen atoms in the structures. Second, we determined the energy of the optimized structure at the MP2/6-311++G(d,p) level. Self-consistent reaction field (SCRF) method were performed on all calculations ($\epsilon=4.24$). Calculations were performed with the NEC SX9 machine equipped with the Gaussian 09 series of programs [18].

The calculated energy value for the rotation of the imidazole between the "in" and "out" conformations can be expressed as a harmonic or parabolic equation (Equation 2),

$$E_n(\chi_1) = \frac{k_n}{2}(\chi_1 - a_0^n)^2 + b \quad (2)$$

where E_n and χ_1 are the harmonic restraining potential (kcal mol $^{-1}$) and the N – C α – C β – C γ dihedral angle (°), respectively. Parameters (the spring constant (k_n) and the coordinate of local minimum point (a_0^n , angle and b , energy)) were determined by fitting Equation 2 to each region of the energy data. The unit of the k_n was converted to the unit, kcal mol $^{-1}$ rad $^{-2}$.

3 Result and Discussion

3.1 Potential Energy Surface of π -stacking Interaction in Relation to Rotational Motion (N $_{\delta 1}$ -H Tautomer)

The calculated energy values were plotted as a function of the χ_1 angle of the His64 N $_{\delta 1}$ -H tautomer to investigate the profile of the π -stacking interaction, as shown in Figure 2A. In order to compare

Model A with Model B, we superimposed two curves of energy data: the "out" conformation (the structure that has the negative value of χ_1 angle) of the imidazole ring of His64 planar parallels to the indole ring of Trp 5 in an off-centered structure (Model A, Figure 1), the imidazole slides out of the off-centered structure to be the "in" conformation (the structure that has the positive value of χ_1 angle (Model B, Figure 1). On this basis, the energy of the π -stacking interaction between the indole and the imidazole in the negative region of χ_1 angle should be lower compared to that of positive region of χ_1 angle. At the high χ_1 angle (positive region), the imidazole ring of His64 and the indole ring of Trp5 is not form planar parallel. There was expected to be the lowest π -stacking interaction energy in the model having the highest χ_1 angle (101.4°, Figure 2(a)) among those of any tested angles. Therefore, the curve of Model B was superimposed on that of Model A at 101.4°, as shown in Figure 2(a). In fact, there is no difference between the spring constant k_n of Model A and that of Model B in positive region, as summarized in Table 1. This indicates that no π - stacking interaction energy between the imidazole and the indole.

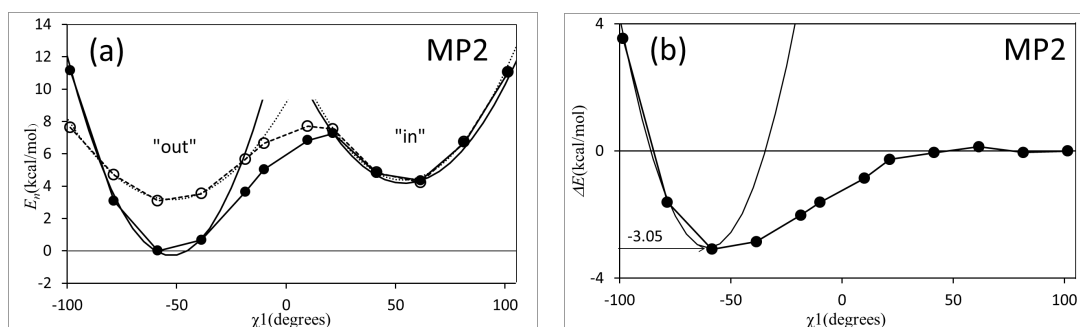


Figure 2: **a.** The χ_1 angle-dependent curves of the His64 $N_{\delta 1}$ -H tautomer within Model A and Model B (MP2 method). The closed circle along the solid line and the open circle along the dashed line refer to Model A and Model B, respectively. The difference between the entire energy value of the model structures and the lowest energy value of the model at -58.6° among twelve points of Model A was used as the calculated energy, E_n . The curve of Model B was superimposed on that of Model A at the 101.4° (see also Result). This energy profile indicates the potential energy surface of rotational motion with and without the π -stacking interaction. Note that the curvature k of the negative region of model A is higher, compared to that of model B, whereas there was no difference in the curvature k of the positive region. **b.** The energy difference between the curves of Model A and Model B ($E_{nA} - E_{nB}$).

Table 1: Parameters of harmonic equation for $N_{\delta 1}$ -H tautomer

		"in" conformation		"out" conformation		
		Model A	Model B	Model A	Model B	A-B
MP2	k_n	20.4	19.04	36.1	14.4	30.2
	(a_n^0, b)	(53.1, 4.08)	(53.7, 4.17)	(-52.0, 0.03)	(-51.6, 2.87)	(-60.3, -3.05)
B3LYP	k_n	23.6	23.6	34.8	13.1	-
	(a_n^0, b)	(52.3, 2.29)	(50.0, 2.26)	(-45.3, 2.07)	(-57.0, 0.25)	-

Parameters (the spring constant (k_n , kcal mol $^{-1}$ rad $^{-2}$) and the coordinate of local minimum point (a_n^0 , angle and b , energy)) were determined by fitting Equation 2 to the energy data.

In the negative region of the χ_1 angle, the energy value at the bottom of curve of Model A was lower than that of Model B, indicating that the indole stabilized the imidazole *via* the π -stacking interaction. This also can be seen by comparing the spring constant k_n of Model A and Model

B. Note that the change of curvature would be a force constant of the π -stacking interaction. In order to tentatively determine the constant of this π -stacking interaction, we subtracted the energy values of Model B from Model A, as shown in Figure 2(b). By fitting the Equation 2 to the data, we can see the π -stacking interaction in relation to the rotational motion of His64. This result indicates that the π -stacking interaction should not be ignored when the rotational motion is assumed to occur in carbonic anhydrase.

The energy surface of each model system appears to have two valleys (the angles at the bottoms of valleys are close to those of the "in" and "out" conformations that are observed in the crystal structure). This profile is consistent with the result obtained by using the model: the zinc ion, Tyr7, Asn62, His64, Asn67, His94, His96, His119, Thr199, Thr200, and several water molecules between His64 and zinc ion (Maupin's model)[9]. However, the electron correlation between Trp5 and His64 was not considered in simulating the model. At the same point of the highest π -stacking interaction at MP2 method (3.05 kcal/mol at -58.6°), the interaction without electron correlation was confirmed when we applied the same method (B3LYP) as Maupin et al. to Model A and Model B, as shown in Figures 3(a) and 3(b). We simply added the energy difference between the "out" conformation of MP2 method and B3LYP (3.05-6.10 kcal/mol) into Maupin's model energy barrier (6.2 kcal/mol). This can increase the energy barrier to 9.25-12.3 kcal/mol. By using this value, the $10^6 s^{-1}$ of the kinetic rate of reaction would not be explained, according to the transition theory.

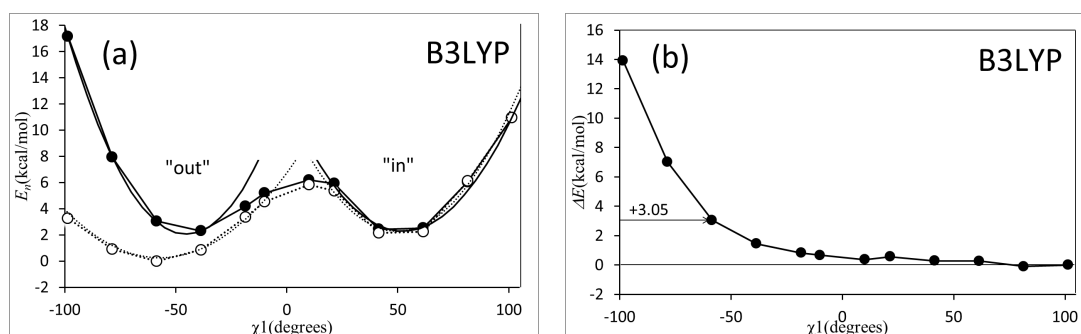


Figure 3: **a.** The χ_1 angle-dependent curves of the His64 $N_{\delta 1}$ -H tautomer within Model A and Model B (B3LYP method). The closed circle along the solid line and the open circle along the dashed line refer to Model A and Model B, respectively. The difference between the entire energy value of the model structures and the lowest energy value of the model at -58.6° among twelve points of Model A was used as the calculated energy, E_n . The curve of Model B was superimposed on that of Model A at the 101.4° (see also Result). Note that the curvature k of the negative region of model A is lower, compared to that of model B, whereas there was no difference in the curvature k of the positive region. **b.** The energy difference between the curves of Model A and Model B ($E_{nA} - E_{nB}$). This indicates no π -stacking interaction between the imidazole and the indole.

4 Conclusion

MP2 calculations allow us to tentatively determine the potential energies of the π -stacking interaction of the $N_{\delta 1}$ -H tautomer of imidazole with the indole in relation to the side chain rotation. The result indicates that the π -stacking interaction causes an increase of the energy barrier of rotational motion. This implies that explaining the proton transfer during catalysis *via* the rotational motion of His64 is not appropriate. Alternatively, a static manner of His64 would be needed.

References

- [1] S. Lindskog, G. Behrvean, C. Engstrand, C. Forsman, B. Jonsson, Z. Liang, X. Ren, and Y. Xue (1991) in *Carbonic Anhydrase from Biochemistry and Genetics to Physiology and Clinical Medicine*, 1 – 13.
- [2] I. Simonsson, B. H. Jonsson, and S. Lindskog (1979). C-13 NMR study of carbon dioxide-bicarbonate exchange catalyzed by human carbonic anhydrase C at chemical equilibrium. *Eur. J. Biochem*, **93**, 409 – 417.
- [3] D. N. Silverman, C. K. Tu, S. Lindskog, and G. C. Wynns (1979). Rate of exchange of water from the active site of human carbonic anhydrase C. *J. Am. Chem Soc.*, **101**, 6734 – 6740.
- [4] T. H. Maren (1967). Carbonic anhydrase: chemistry, physiology, and inhibition. *Physiol. Rev.*, **47**, 595 – 781.
- [5] R. E. Tashian (1989). The carbonic anhydrase: widening perspectives on their evolution, expression and function. *BioEssays*, **10**, 186 – 192.
- [6] H. Steiner, B. H. Jonsson, and S. Lindskog (1975). Catalytic mechanism of carbonic-anhydrase-hydrogen-isotope effect on kinetic-parameters of human C isoenzyme, *Eur. J. Biochem*, **59**, 253 – 259.
- [7] C. K. Tu, D. N. Silverman, C. Forsman, B. H. Jonsson, and S. Lindskog (1989). Role of histidine 64 in the catalytic mechanism of human carbonic anhydrase II studied with a site-specific mutant. *Biochemistry*, **28**, 7913 – 7918.
- [8] K. Hakansson, M. Carlsson, L.A. Svensson, and A. Liljas (1992). Structure of native and apo carbonic anhydrase II and structure of some of its anion-ligand complexes. *J. Mol. Biol.*, **227**, 1192 – 1204.
- [9] C. Maupin and G. A. Voth (2007). Preferred orientation of His64 in human carbonic anhydrase II. *Biochemistry*, **46**, 2938 – 2947.
- [10] D. N. Silverman and R. McKenna (2007). Solvent-Mediated Proton Transfer in Catalysis by Carbonic Anhydrase. *Acc. Chem. Res.*, **40**, 669 – 675.
- [11] D. Riccardi, P. Knig, H. Guo, and Q. Cui (2008). Proton Transfer in Carbonic Anhydrase Is Controlled by Electrostatics Rather than the Orientation of the Acceptor. *Biochemistry*, textbf47, 2369 – 2378.
- [12] H. Shimahara, T. Yoshida, Y. Shibata, M. Shimizu, Y. Kyogoku, F. Sakiyama, T. Nakazawa, S. Tate, S. Ohki, T. Kato, H. Moriyama, K. Kishida, Y. Tano, T. Ohkubo, and Y. Kobayashi. (2007). Tautomerism of Histidine 64 Associated with Proton Transfer in Catalysis of Carbonic Anhydrase. *J. Biol. Chem.*, **282**, 9646 – 9656.
- [13] R. L. Mikulski, D. West, K. H. Sippel, B. S. Avvaru, M. Aggarwal, C. K. Tu, R. McKenna, and D. N. Silverman,(2013). Water Networks in Fast Proton Transfer during Catalysis by Human Carbonic Anhydrase II. *Biochemistry*, **52**, 125 – 131.
- [14] M. Koyimatu, H. Shimahara. M. Iwayama, K. Sugimori, K. Kawaguchi, H. Saito, and H. Nagao (2012). Theoretical model for assessing properties of local structures in metalloprotein. *AIP Conf. Proc.*, **1518**, 626 – 629.

- [15] C. Lee, W. Yang, R. G. Parr (1988). Development of the Colle-Salvetti correlation-energy formula into a functional of the electron density (1987). *Phys. Rev. B*, **37**, 785 – 789.
- [16] C. Møller, and M.S. Plesset (1934). Note on an Approximation for Many-Electron Systems. *Phys. Rev.*, **46**, 618.
- [17] P. C. Hariharan, and J. A. Pople (1973). The Influence of Polarization Function on Molecular Orbital Hydrogenation Energies. *Theor. Chim.*, **28**, 213 – 222.
- [18] Gaussian 09, Revision A.1, M. J. Frisch, G. W. Trucks, H. B. Schlegel, G. E. Scuseria, M. A. Robb, J. R. Cheeseman, G. Scalmani, V. Barone, B. Mennucci, G. A. Petersson, H. Nakatsuji, M. Caricato, X. Li, H. P. Hratchian, A. F. Izmaylov, J. Bloino, G. Zheng, J. L. Sonnenberg, M. Hada, M. Ehara, K. Toyota, R. Fukuda, J. Hasegawa, M. Ishida, T. Nakajima, Y. Honda, O. Kitao, H. Nakai, T. Vreven, J. A. Montgomery, Jr., J. E. Peralta, F. Ogliaro, M. Bearpark, J. J. Heyd, E. Brothers, K. N. Kudin, V. N. Staroverov, R. Kobayashi, J. Normand, K. Raghavachari, A. Rendell, J. C. Burant, S. S. Iyengar, J. Tomasi, M. Cossi, N. Rega, J. M. Millam, M. Klene, J. E. Knox, J. B. Cross, V. Bakken, C. Adamo, J. Jaramillo, R. Gomperts, R. E. Stratmann, O. Yazyev, A. J. Austin, R. Cammi, C. Pomelli, J. W. Ochterski, R. L. Martin, K. Morokuma, V. G. Zakrzewski, G. A. Voth, P. Salvador, J. J. Dannenberg, S. Dapprich, A. D. Daniels, ?. Farkas, J. B. Foresman, J. V. Ortiz, J. Cioslowski, and D. J. Fox, Gaussian, Inc., Wallingford CT, 2009.